INSTRUMENTATION

Progress in the Detector Laboratory

J. Yurkon, B. Lynch, and B. Jacak

Improvements have been made in the detector laboratory facility including a 40 inch test chamber, addition of a camac based data acquisition facility, addition of a 18 inch bell jar test stand, construction of a ecl/nim converter for use with the PCOS-III system, construction of an improved gas handling system, and a light tight test chamber for evaluation of scintillation detectors and other photo-optical devices. Continuing efforts are being made to improve various techniques used in construction of detectors such as stretching of thin windows, metalizing of windows, and improvement of the wire winding machine. Various detectors have been designed and others are undergoing continuing testing. These will be reported on separately in this paper by the individuals involved. Included are a counter system, called the P212 for the S320 spectrograph consisting of two position sensitive proportional counters and two ionization chambers, a drift chamber for inclusion in the P212, a two dimensional detector for the RPMS that uses drift time and resistive charge division, a two dimensional multiwire proportional counter, an ion chamber for use with an avalanche counter, a Breskin type avalanche counter for fast start timing, a multi-inclined wire detector for the Enge split pole spectrograph, and a position sensitive parallel plate avalanche counter.

The 40 inch scattering chamber has been moved to the detector laboratory for use as a test chamber. It was necessary to have a base plate, a stand and various cover plates machined. The well was cut to a short height above the floor to allow the 40 inch chamber to roll into place over it. The well can still be accessed as the chamber is now on casters. The vacuum system consists of a large mechanical roughing pump with a molecular sieve to prevent backstreaming of oil, a CTI-Cryogenics cryopump, an ion gauge and thermocouple gauge for pressure readout. A vacuum of approximately 2.0×10^{-7} torr has been achieved in a 12 hour time period.

A camac based data acquisition facility is being added to the detector lab to allow the testing of detectors when multi-parameter type analysis is necessary. At present it will consist of one camac crate and controller directly interfaced to the VAX 11/750. Data display and program control will be via a DEC UT100 terminal with Retro-Graphics model UT 640 enhancement modification. At a later date a camac style LSI 11/23 may be added if experience indicates a need.

An 18 inch bell jar with stand has been added so that detectors that have been built, but that do not yet have a case, can be tested and be visible during testing. The stand has a gas feed through port for connection to the gas handling system, and two connector plates with various styles of connectors.

Testing of the MIW detector and the Multiwire Proportional counter required that a differential ecl to nim standard converter be built since as of yet LeCrory does not yet have a PCOS-III controller through production. The ecl/nim converter has 16 differential ecl inputs via a standard 34 pin header for use with twisted pair cable and 16 standard nim outputs via lemo connectors. The converter allows the amplifiers discriminators cards to be read out through a standard coincidence register, but may be used for other applications.

A new electronic gas handling system has been constructed since it was discovered that one alone is inadequate for the number of detectors being built. It is based on the Datametrics type 1404a valve controller in conjunction with a Datametrics 1400 Electronic manometer and Type 590 barocel sensor, the flow control valve is a Brooks solenoid valve. The unit was constructed with portability in mind and is enclosed in a standard chassis. For use with low pressure detector it was apparent that large diameter tubing and valves should be used for minimal pressure drops. KF-15 vacuum fittings are used for that reason and ease of assembly. KF-15 Balzer quarter turn valves are used throughout and a hermetic bellow sealed needle valve for rate of flow. A flowmeter indicates rate of flow over two ranges, the electronic manometer displays the pressure, and a thermocouple gauge is installed to help indicate leak problems. The controller appears to be stable even when controlling large volumes and pressures down to less than 0.5 torr.

A 28" x 28" x 13" light tight box has been constructed for testing of photo sensitive devices. It has BNC and SHV feedthroughs plus 110 VAC. The lid can be completely removed to allow for complete access. It has been useful in testing the new light pipe for the plastic scintillator that will sit behind the P212 detector on the S320 spectrograph.

Thin polypropylene windows in the 50 to 70 microgram cm/2 range have been stretched on the foil stretcher and used in parallel plate avalanche counters. Thinner foils have been made but not with reproducibility and they have not been accurately measured. Further work is being done to develop techniques to produce thin foils. Irregularities in the unstretched material seem to be the main difficulty at present that makes producing extremely thin foils difficult.

To use the polyproylene windows as electrodes in counters requires that they be metalized. We have tried evaporating gold, silver, aluminum, and gold paladium alloys. Gold and silver are the easiest and can be deposited in any required thickness. However, to achieve high surface conductivity requires a large mass thickness due to their high Z. Also silver tends to oxidize in time. Aluminum is the prime choice since it has a low Z and is resistent to oxidation. It can also be etched after evaporation whereas gold cannot. To date we have produced aluminized polypropylene windows of the 50 to 70 microgram range with a surface conductivity of down to 10 ohms/square. The most effective method to date is evaporation from a coiled tungsten wire. Other techniques such as electron gun evaporation are being tried. The 40" test chamber is being set up for evaporation of large areas and will be used for most of the further tests.

The wire winding machine has had its program revised to allow it to stop upon wire breakage or the spool tangling. A further improvement to be made are to paint or anodize various parts of it black to improve visibility of the fine wires used.

Response of Bismuth Germanate to Monoenergetic Gamma-rays

D. J. Morrissey

A new scintillation material has become available for large volume gamma-ray detectors. The material is bismuth germanate ($Bi_3 Ge_4 O_{12}$;BGO). BGO has attracted attention on the basis of its relatively high density (7.13 gm/cm^3) as compared to NaI(Tl) (3.67 gm/cm^3) and its high stopping power due to the presence of the bismuth in the crystal lattice. The new material has its own drawbacks in that it has a scintillation light output that is only 8 percent of that of NaI(Tl) and also has a higher index of refraction than NaI(Tl), 2.1 relative to 1.85 at the respective spectral peaks. These properties taken together make BGO a scintillation material that will be more efficient at stopping a gamma-ray in a given volume but will have an inherently poorer resolution than the comparable NaI(Tl) scintillator. The initial applications of BGO scintillators have been ones in which resolution is not a factor, e.g. in positron cameras for nuclear medicine or as anti-Compton shields for germanium detectors. Another area where BGO could be used to advantage is continuum gamma-ray spectroscopy of heavy-ion reactions. In such studies the resolution need not be optimal but rather the fraction of the events that lie in the photopeak should be maximized. Previous continuum gamma-ray studies using NaI(Tl) detectors have been hampered by the necessity of unfolding the response function of the detectors and by the sensitivity of the detectors to neutrons created during the nuclear reaction.

In preparation for continuum gamma-ray experiments at NSCL a prototype BGO detector was obtained from the Harshaw Chemical Company. The detector was cylindrical 7.6 cm x 7.6 cm integrally coupled to a Hamamatsu R-1307 photomultiplier tube. The resolution and the peak to total ratio of the detector were calibrated by a coincidence technique using radioactive sources that emit a pair of gamma-rays in cascade (e.g. ^{60}Co, ^{94}Nb, etc.). An intrinsic Ge detector acted as the trigger for a fast coincidence circuit that recorded the BGO pulse height of the other cascade gamma-ray. This system avoided contamination from the rather substantial background in the BGO that would be seen in a singles measurement (The detector had an average background counting rate of approximately 0.05 counts/sec/keV in the range of 0 to 3 MeV.)

The results of resolution measurements are shown in Fig. 1. They are comparable to previous measurements of smaller BGO crystals,[1] the straight line indicates that the resolution is dominated by the statistics of the photoelectrons emitted from the photocathode. The peak to total measurements show that the detector reaches a maximum of approximately 90 percent below 600 keV and falls gradually to 70 percent at 1500 keV. Further measurements with higher energy gamma-rays are continuing.

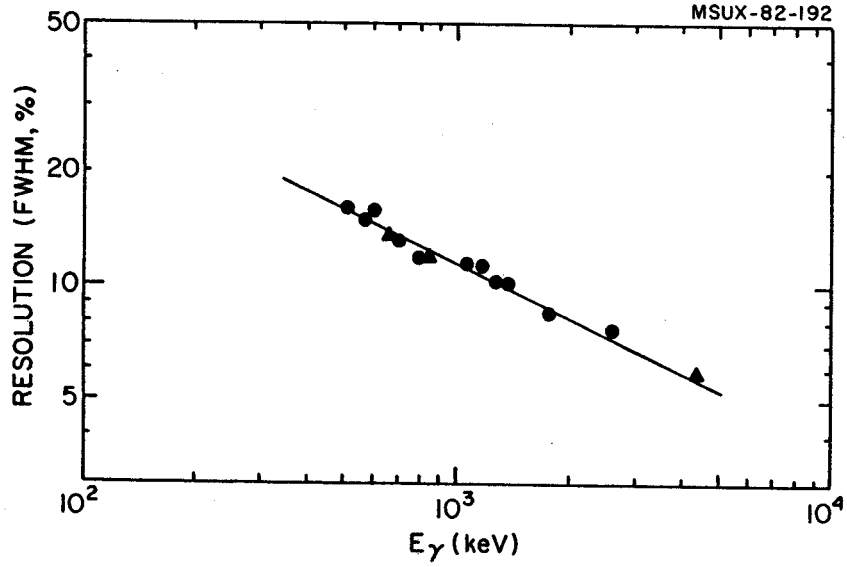

Fig. 1. The resolution of a 7.6 cm x 7.6 cm BGO detector is shown as a function of gamma-ray energy. Circles indicate the results from coincidence measurements and triangles the results from singles measurements.

1. A.E. Evans, IEEE Trans. Nucl. Sci. NS-27 (1981) 172.

Design Studies for a Multielement High Resolution Anti-Compton Shielded Detector Array (MEHRACS)

J.X. Saladin,* C. Baktash,** I.Y. Lee,** R. Blue, R. Ronningen and R.A. Sorensen+

A detailed study of the performance characteristics of a gamma-ray facility for the investigation of high spin phenomena was made.

The proposed device combines an array of anti-Compton shielded intrinsic-Ge detectors with a multiplicity and total energy spectrometer. The proposed device is shown in Figure 1 and combines an array of high resolution detectors with a multiplicity and total energy spectrometer. It will permit us to perform high resolution energy-energy correlation experiments (2-fold coincidences) as well as triple energy correlation experiments (3-fold coincidences) at a large event rate and hence with good statistics. Of pivotal importance for such experiments is a large peak-to-total ratio which is achieved through the use of anti-Compton shielded Ge detectors. The performance of the anti-Compton shield is presently being investigated in detail by means of a Monte Carlo code made available to us by F.T. Avignone (University of South Carolina). The result of a sample

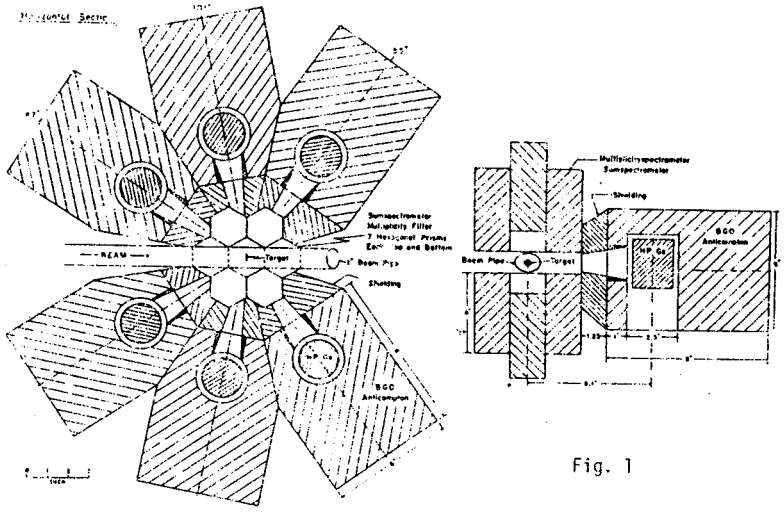

Fig. 1

calculation (for monoenergetic γ-rays of 2 MeV) is shown in Figure 2. It is evident that the proposed anti-Compton shields result in an average Compton suppression of 16 for 2 MeV γ-rays. The peak-to-total ratio increases from .17 for the bare detector to .67 for operation with the anti-Compton shield. At present, calculations are being performed at various energies and we are investigating the effects of changes in geometry.

The device makes extensive use of the new bismuth germanate (BGO) technology. The absorption coefficient of BGO is on the average a factor of 2.2 times larger than that of NaI. BGO detectors can therefore be considerably more compact than comparable NaI detectors. Because of this, it is possible to surround the target with a highly effective multiplicity total-energy spectrometer. BGO also permits a very compact design for the anti-Compton shields. This results in a large solid angle (.8% of 4π) for the individual detectors and makes it possible to position six detectors around the target.

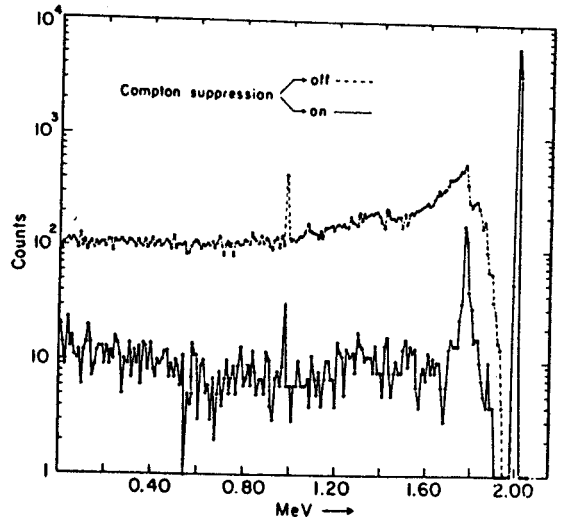

Fig. 2.

* University of Pittsburgh
** Oak Ridge National Laboratory
+ Carnegie-Mellon University

The Pulse-Height Correction Technique for Improving γ-Ray Spectra From Coaxial Ge Detectors

N. Matsushita, J. Kasagi and Wm. C. McHarris

The pulse-height correction (PHC) technique,[1] is a means by which one can improve both the energy resolution and the peak-to-Compton ratios of γ-ray spectra taken by Ge detectors. To do so one performs a detailed analysis of the rise-times of the pulses coming from the detectors. In general, pulses having slower rise-times are associated with damaged or defective portions of the detector; consequently, these pulses suffer from incomplete charge collection. Thus, merely by "throwing away" such slower rise-time pulses, one can immediately improve the resolution, albeit with a significant loss in detector efficiency.

With PHC one can circumvent this loss in efficiency in the following manner: the spectra can be sorted into bins or slices as a function of the pulse rise-time. If a correlation can be found between the rise-time and the degree of incompleteness of charge collection, then a correction can be made to compensate for the incompleteness of charge collection. Each bin or slice can be corrected in turn, and many or most of the corrected slices can be reassembled to produce an improved spectrum characteristic of a superior detector. And this can be done without any significant loss in detector efficiency.

As might be expected, the PHC method produces its most dramatic results with Ge or Ge(Li) detectors whose resolution has deteriorated, most often because of neutron damage. For such detectors we have obtained resolutions improved by 40-50% - and this was done more or less routinely, using electronics that are available in most nuclear science or counting laboratories. For pristine, state-of-the art, highest-resolution intrinsic Ge detectors, results from the PHC technique are much less dramatic - indeed, they can become marginal to the point that it is not worth the bother of applying the technique. However, most laboratories have γ-ray detectors that are no longer of the highest quality, yet which are too good to discard or to send back for refurbishing. Since the PHC technique is basically a straightforward process, it can be quite useful in improving the quality of the spectra obtainable from these middle-quality detectors.

For coaxial, trapezoidal, and other detectors having "nonsimple" geometries, a complication arises: The electric field in such detectors is no longer uniform, and this in itself introduces a variation in the rise-time of a pulse that is geometry dependent, i.e., depends on where in the detector the photon interaction takes place. Thus, even undamaged, highest quality coaxial detectors in which there is complete charge collection for each and every event still exhibit a range of pulse rise-times.

An experimental illustration of the problems incurred in correlating rise-times with pulse-height defects is given in Fig. 1. Here the pulse-height spectrum of the ^{60}Co 1332.513-keV peak is shown as a function of rise-time. It can be seen that not only does the peak broaden with increasing rise-time, but also it splits into a doublet, the lower-energy component of which shifts in position. No longer can one make a straightforward assignment of the lower-energy component to incomplete charge collection and the higher-energy component to relatively complete charge collection.

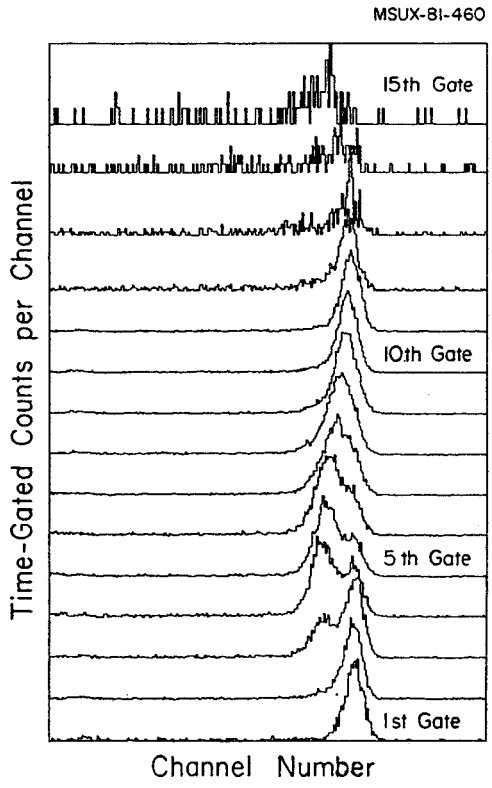

Fig. 1. Correlation between pulse rise-time and pulse-height for the ^{60}Co 1332.513-keV peak in a spectrum taken by a ≈16%-efficient true-coaxial Ge(Li) detector. The spectra shown are time-gated slices, with the fatest rise-time in the first gate, then progressively slower ones until the slowest is reached in the fifteenth gate.

Since a complete analysis of these rise-time and trapping phenomena are beyond the scope of the present experiments, what we are seeking is a moderately simple, empirical approach to

the correlation between rise-time and pulse-height defect. This can be found by analyzing the rise-times of two pulse segments: Suppose we were to use three constant-fraction timing discriminators to analyze the pulse rise-times, setting them, for example, at 0.1, 0.5, and 0.7 fractions of the rise-times. Now, a "good" pulse having complete charge collection but originating from a portion of the detector with a geometrically slow rise-time just might have, say, the same 0.1-0.5 fraction rise-time as a "poor" pulse slowed down by trapping and with incomplete charge collection but originating with a geometrically faster rise-time. The two pulses can accidentally have the same rise-time over one fractional interval, but it is highly unlikely that they would have the same rise-time over another interval, for example, that of the 0.1-0.7 fractions. Thus, a double analysis could separate and sort such pulses.

In Fig. 2, we show a block diagram of the electronics for a triple-correlation experiment. All data were recorded event by event on magnetic tape for later recovery and off-line analysis. This was done as follows: Because of limitations in the sizes of computer memory, it is necessary to choose limited portions of the spectra for analysis in a given pass. As an example, for a single analysis we first sorted those portions of the pulse-height spectrum that contained the 244.692-(^{152}Eu), 661.649-(^{137}Cs), 1173.238-(^{60}Co), and 1332.513-keV(^{60}Co) γ-rays and obtained them as a function of both rise-time segments. For the 0.1-0.5-fraction TAC output (hereafter referred to as t_1) we set windows in 1.5-ns steps, and for the 0.1-0.7-fraction TAC(t_2) in 3.3-ns steps.

An example of the variation of the pulse-height spectrum of the 1332.513-keV γ-ray with the t_1 window centered at 37 ns and the t_2 window progressing from 58 to 84 ns is shown in Fig. 3. The lowest spectrum in the figure is the one without t_2 windows, and it shows two broad peaks. The lower of these peaks corresponds to incomplete charge collection from neutron-damaged portions of the detector. As can be seen, this component can be easily separated from the "nondamaged" component by including the t_2 windows. The centroid channel of this component decreases with increasing t_2 value. Thus, it is demonstrated that one can distinguish between "damaged" and "nondamaged" events that have the same rise-time over one fraction by setting gates on another rise-time fraction.

The simplest method for obtaining an improved spectrum is merely to discard the "damaged" events by setting the appropriate two-parameter windows on the rise-time segments. We have done this, with the result that the energy resolution was improved to 2.6 keV fwhm by retaining 10% of the events and to 3.0 keV fwhm by retaining

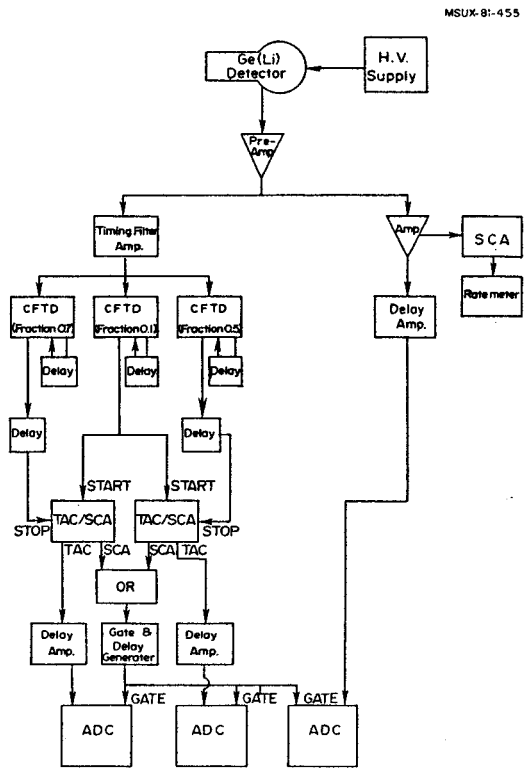

Fig. 2. Block diagram of the circuit used for rise-time discrimination on γ-ray pulses from a single detector. The three ADC's, from left to right, yield, respectively, the analyzed 0.1-0.7-fraction TAC signal, the 0.1-0.5-fraction TAC signal, and the pulse-height signal to be listed on magnetic tape for later off-line three-parameter analysis.

28% of the events. However, the fact that the energy resolutions of the individual gated spectra, even the "damaged" portions, are in general considerably better than that of the raw spectrum makes it possible to obtain the improved spectra without any appreciable loss in efficiency, as was demonstrated for the simpler case of planar detectors in our previous work.[1]

The amount of pulse-height defect resulting from the incompleteness of charge collection is expected to be proportional to the energy of a γ-ray. In other words, the gains of the individual gated spectra are no longer all the same but depend on the two rise-time segments. Therefore, we can fit the centroids of the γ-ray peaks, sorted according to the two rise-time segments, by the simple equation,

$$\varepsilon_\gamma = \alpha(t_1,t_2)x + \beta ,$$

where ε_γ is the energy of the γ-ray, x is the channel number of its centroid, and α and β are parameters to be determined empirically.

In order to generate the improved spectrum, the values of the matrix $\alpha(t_1,t_2)$ and the constant were stored in computer memory, and the corrected energy of each event was calculated

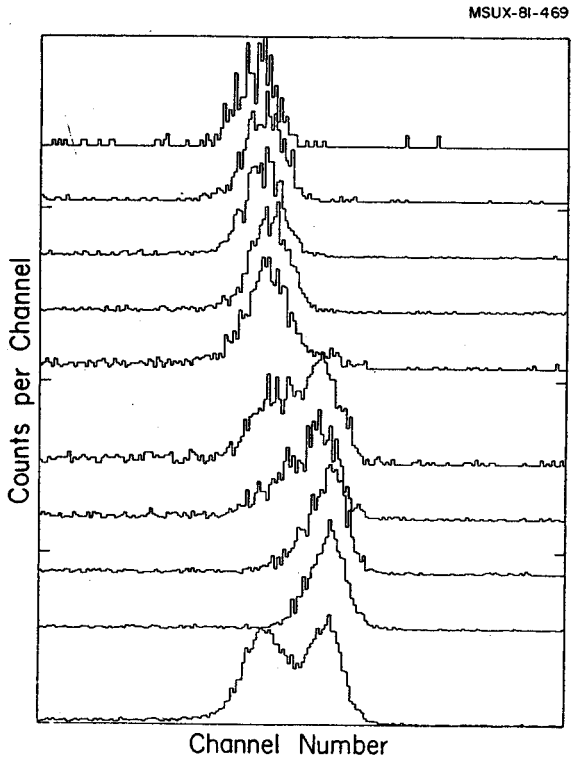

Fig. 3. Example of triple correlation between the pulse-height for the ^{60}Co 1332.513-keV peak and the rise-time for two separate pulse segments. For these spectra the window of the 0.1-0.5 fraction was held constant, while that of the 0.1-0.7 fraction was varied. The bottom spectrum has no gate at all included for the 0.1-0.7 fraction; the second spectrum has the fastest rise-time from this fraction, and this rise-time becomes progressively slower toward the top spectra.

using these values. The final reconstructed spectrum is shown in Fig. 4. The energy resolution of the 1332.513-keV peak was improved from 4.92 to 2.91 keV fwhm and from 8.98 to 6.21 keV fwtm. The peak-to-Compton ratio was improved by about 43%. We emphasize that these improvements were obtained without significant loss in detector efficiency.

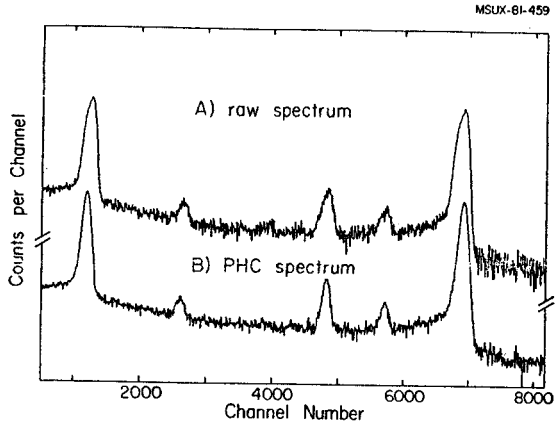

Fig. 4. γ-ray spectra for ^{60}Co + ^{137}Cs + ^{152}Eu sources taken with a 16%-efficient true-coaxial Ge(Li) detector. A) The raw spectrum, with energy resolution of 4.92 fwhm for the ^{60}Co 1332.513-keV peak. B) Pulse-height corrected spectrum, with energy resolution improved to 2.91 fwhm and the peak-to-Compton ratio improved by ≈43% all without significant loss in detector efficiency. (Vertical scales arbitrarily displaced for clarity of display.)

1. N. Matsushita, Wm. C. McHarris, R.B. Firestone, J. Kasagi, and W.H. Kelly, Nucl. Instr. and Meth. 179 (1981) 119.

A Counter System for the S320 Spectrograph

J. Yurkon, B. Lynch and N. Matsushita

A counter system (P212) for the S320 has been constructed and is undergoing preliminary tests. It basically consists of a stack of a position sensitive proportional counter followed by an ionization chamber followed by another SWPC and ionization chamber. These will reside in a common gas volume (Photograph 1.). At the end of the detector case there will be a plastic scintillator for total energy information and timing.

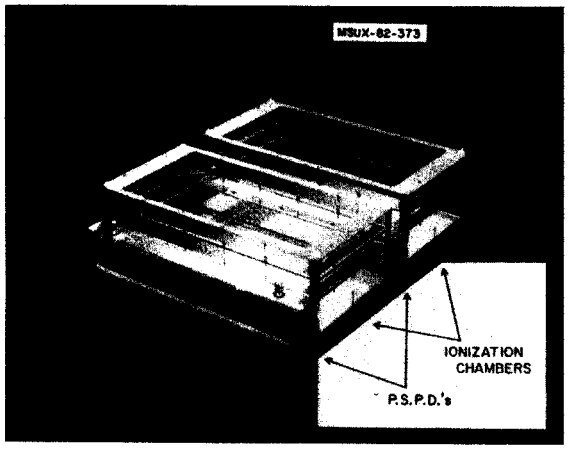

Phot. 1.

The SWPC's are electrically isolated from the ion chambers to prevent the large signals they generate from being coupled to the ionization chamber where the signal levels are quite small in comparison. They are modular units that can be removed for repair or replacement with the drift chambers that are being built. In addition, since they are separate from the ion chambers, they can have a well defined geometry permitting good position resolution. They have an active area of 10" x 1-3/4" and a depth of 1". The width is sufficiently large to extend beyond the lateral limits of the focal plane to provide good linearity at the lateral limit. At this time only very preliminary testing has occurred. Using an Am241 source and a gas pressure of 90 torr or isobutane, the signal to noise ratio measured implies a position of better than 300 microns.

The ionization chambers are of an unusual design in that they do not use a continuous plane for the anode. Instead, we have opted to use a wire anode. Using a wire anode allows the ion chamber to be run with a small amount of gas gain increasing the signal to noice resolution greatly. For separation of lightly ionizing particles, such as ^{6}He and ^{6}Li, the signal to noise ratio may be a limiting factor. By optimizing the gain, energy resolution performance is better than what could be expected for an ion chamber of this size. The ion chamber is 13" wide and 6" deep. The cathode is a flat plate of aluminum of these dimensions. There are three grids above the cathode. The first two have a wire spacing of 1 mm and the third (anoded) grid, has a wire spacing of 1 cm. The first two grids provide a faraday cage that performs the function of a Frisch grid. In this configuration the signals from the faraday cage could be used in place of the anode signals. This might be a preferred configuration for detectors of heavily ionizing particles such as ^{40}Ar where signal to noise considerations are not the dominant factor in energy resolution as gas gain of 6.6 was chosen for these measurements. The first grid is 1.75 inches above the cathode plain and the next two grids are spaced 1.0 inches each.

Energy resolution tests have been performed using the 5.4 MeV alpha of Am 241 and the 6.0 and 8.8 MeV alphas of Pb 212 at gas pressures of 250 torr and 550 torr respectively. A canberra 2001A preamplifier was used and the spectroscopy amplifier was set for an intergation time constant of 2.0 microseconds. The gas pressures chosen were sufficient to completely stop the alphas in the ionization chamber. For these tests, it was necessary to collimate tightly to ensure that the particles stopped in the active volume of the ion chamber. The observed energy resolution for Am 241 was 61 keV. Correcting for the 55 keV of straggling due to the 1.25" dead layer in the alpha source colimator gives a ion chamber resolution of 25 keV. Using the Pb 212 source gas an observed delta E.F.W.H.M. of 86 keV for the alphas. At the higher pressure of 550 torr, the straggling in the dead layer was 81 keV giving an ion chamber resolution of 29 keV.

A Two-Dimensional Counter for the RPMS

E. Ormand, J. Nolen and J. Yurkon

A two-dimensional heavy-ion detector is being developed to compare the focal plane characteristic of the reaction products mass separator with calculations performed with the Transport, Ray Trace, and Motor programs. The detector consists of a drift region and a proportional counter region as shown in Fig. 1. The ionized electrons dirft through the 5000 volt gradient and are collected on the proportional counter wire. A second induced signal is them observed on the timing grid. The deciphering of the heavy-ion position will be performed by resistive charge division on the propertional wire for the horizontal position, while the vertical position will be determined by measuring the time difference between a start signal producedby the heavy-ion in a scintillator behind the detector and a stop signal produced on the timing grid. In the drift region the electric field gradient will be approximately 1000 volts/cm which is produced by a series of voltage dividers and field shaping wires as shown in Fig. 1. The detection area is approximately 6.2 cm x 5.2 cm. At present the resolution of the detector is being determined with a collimated α source and a collimated Si barrier detector.

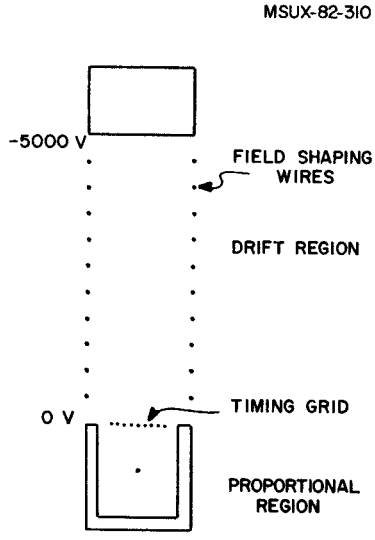

Fig. 1.

A Fast Start Detector for Heavy Ions

J. Yurkon, B. Lynch, A. Galonsky, B. Remington

A fast start detector is being built to provide fast start timing for heavy ions with a time resolution of better than 200 pico seconds. The detector will have an active area of 1.8" by 1.8". The detector will have a wire anode plane with a wire spacing of 1 mm of 12 micron gold plated tungsten. The cathode planes will be spaced 0.125 inches from the anode. This geometry give a field distribution such that the counter operates in a regime between that of a proportional counter and a parallel plate counter. The parallel plate aspect gives good timing and the proportional counter aspect gives sufficient gain for the small energy losses desired. The counter is expected to be operated with a gas pressure of .5 torr of isobutane or hexane. Both the cathode electrodes and the gas pressure windows will be made of stretched polypropylene in the 50 microgram/cm**2 range. The frames that hold the wires and windows will also form an integral detector case so that the width of one edge of the detector case so that the width of one edge of the detector can be held to 0.156" or less. With two pressure windows, two cathodes, and 0.5 inches of 0.5 torr of isobutane the detector will have a mass thickness of 400 micrograms/cm**2.

An Ion Chamber for Use With An PPAD

J. Yurkon and B. Lynch

An ion chamber is being built using a detector case for a PPAD described elsewhere in the annual report. The ion chamber will have two cathode planes with a anode plane sandwiched in between. To eliminate position dependence of the signal the two cathode signals will be subtracted from the anode signal. To reduce the degradation in the signal to noise ration due to capacitive loading on the preamplifier, low noise amplifiers that can be mounted in the detector itself are being designed.

Construction of Position Sensitive Parallel Avalanche Counters

J. Yurkon, M.B. Tsang, W.G. Lynch, Z.R. Xu, G. Poggi, L.W. Richardson and C.K. Gelbke

Parallel plate avalanche counters (PPAC's) have been developed by a number of nuclear physics groups for exclusive measurement of heavy fragment production in heavy ion reactions.[1-5] These detectors offer large solid angle, high count rate capability, 100% detection efficiency without radiation damage problems caused by heavily ionizing fragments in their solid state counterparts. The detectors are reliable, easily constructed, provide x-y position measurement and time-of-flight mass identification with a minimum of electronics. We report here the development, construction and preliminary testing of two large area position sensitive parallel plate avalanche counters. These detectors are a modified design to a prototype we have previously reported.[6]

The detectors consist of two parallel 1.5 m metalized polyester foils with an active area of 16 cm x 20 cm separated by a 3 mm gap over which is applied a large homogeneous electric field. The pressure of the multiplication gas in the detector is regulated to $\pm$0.10 torr by MKS precision solenoid valves and controller. The gas between the plates is replenished by a forced flow rather than a diffusive flow as used in the earlier prototype. This modification was necessary to prevent breakdown of the electric field during extended periods of operation.

The avalanche resulting from passage of an ionizing particle induces a fas negative pulse on the anode with a rise-time of 2 ns. This signal is amplified externally and is used to provide a timing signal with constant fraction discrimination. Position measurement is obtained by the interpolating delay-line technique of ref. 1. A sense grid consisting of a wire plane with a 2 mm spacing is placed between the anode and cathode planes at half of their potential difference. A position signal is induced on the wires by the avalance and the corresponding position is determined by measuring the time difference between the arrival of the induced pulse at the two ends of the delay line, thus alleviating the requirement for an amplifier and discriminator at each wire. The LC delay line employed consists of Rhombus 10 tap integrated circuits which were presorted for values within 21.3 $\pm$ 0.3 ns and arranged according to value to minimize nonlinearity.

The PPAC itself consists of two of the above units for measurement of two orthogonal position coordinates and is contained in an aluminum housing with 65 $\mu g/cm^2$ propylene windows. The housing is designed for transmission mode use so that the detector may be coupled to an array of solid state counters or a gas proportional counter for energy measurements.

The two PPAC units have been fully assembled and testing is in progress. The counters are being operated at a reduced field of up to 500 volts/torr; cm with isobutane and have a position resolution of 1 mm or better.

---

1. D.V. Harrach and H.J. Specht, Nucl. Inst. Meth. 164, 477 (1979).
2. Y. Eyal and H. Stelzer, Nucl. Inst. Meth. 155, 157 (1978).
3. J. Van der Plicht, Nucl. Inst. Meth. 171 43 (1980).
4. H. Lynen, H. Stelzer, A. Gobbi, H. Sann, and A. Olmi, Nucl. Inst. Meth. 162, 657 (1979).
5. M. Just, D. Habs, V. Metag and H.J. Specht, Nucl. Inst. Meth. 148, 283 (1978).
6. M.B. Tsang, et al., MSU Cyclotron Lab Annual Report, 1980-81.

M.I.W. Proportional Counter

K. Beard, E. Kashy, J. Yurkon, W. Benenson

Experiments to measure the pion energy spectrum from (HI,π) reaction below the nucleon-nucleon pion production threshold using the Enge split pole spectrograph require the development of a new multiwire gas proportional counter. This detector has been designed to solve two problems; 1) the very high background which is expected from the high intensity high energy beam and 2) the 45° incidenced angle on the focal plane which makes the conventional MWPC configuration cumbersome.

The multi-inclined wire (MIW) counter solves this by positioning the wires along the trajectory direction (fig. 1). The energy loss signal from the nearly minimum ionizing particle is therefore optimized relative to the randomly directed background events. At most three wire can fire, which is an appreciable improvement over the 9 expected from the conventional MWPC configuration at 45° incidence. MWPC's in general are required to minimize the active volume per output channel. In other words a single wire counter would have a raw counting rate (all background) in the preamp 100 times larger than each wire of 100 wire MWPC.

The new LeCroy PCOS III system will connect each anode wire to its own amplifier/discriminator and hence to CAMAC and the VAX 750.

The prototype counter (Fig. 2), with 32 active wires, has a primary cathode-anode gap of .353", a secondary cathode-anode gap of .062", and a wire spacing of .0707". The wire is 12.7 um gold plated tungsten, and the gas is 50-50 argon-ethane at atmospheric pressure.

Currently, the prototype is being run at -4.53 KV on the primary cathode, -1.51 KV on the secondary cathode, and the anode at ground. Tests using collimated 3.54 MeV electrons from a Ru-106 source, triggered by a plastic scintilator behind the detector, have shown that about 90% of the time only one wire will fire. The distribution of firings per wire is shown in Fig. 3. The spread in the distribution is due to multiple scattering of the electrons, as only 5 wires lie along the path defined by the collimator. Also shown is a histogram of number of wires fired per event verses the number of such events. The current pulses are about 10 uA. Operating at higher voltages increases the size of the signal by more than a factor of 10. The amplifiers saturate before the MIW starts sparking.

Modifications currently underway include doubling the wire spacing and placing a second MIW immediately behind the first (within the same gas box) in order to improve rejection of spurious events.

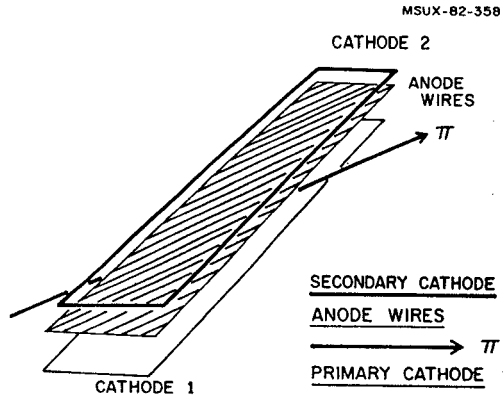

Fig. 1. MIW configuration.

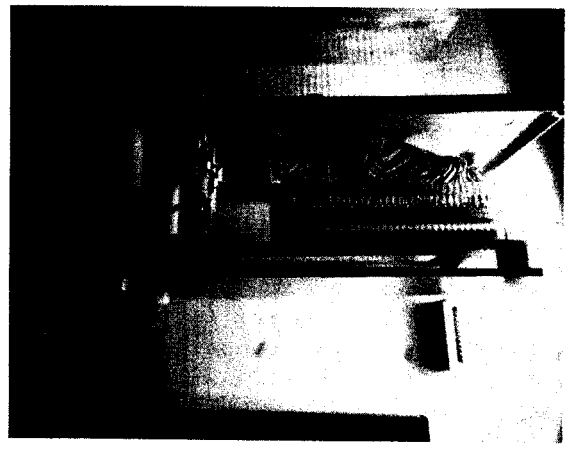

Fig. 2. MIW prototype II.

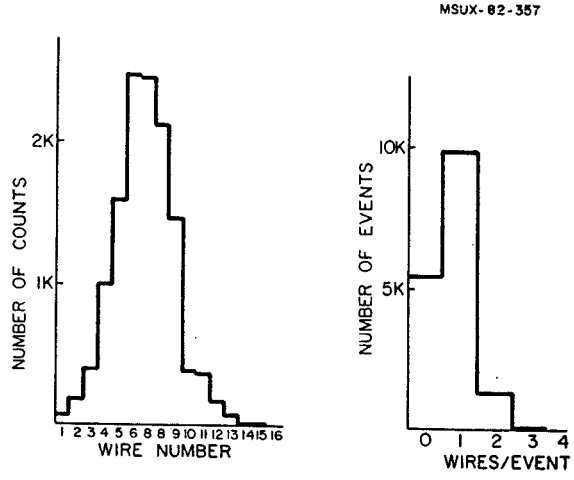

Fig. 3. Behavior of prototype MIW.

Construction of a Multiwire Proportional Chamber

B. Tickle, B. Hasselquist, G. Crawley, B. Tsang and J. Yurkon

A prototype multiwire proportional chamber (MWPC), similar to concept to those which have been used for many years in high-energy physics, has been designed and constructed for use in the 60-inch scattering chamber. Detectors of this type will probably find increasing application in heavy-ion physics as they provide excellent position resolution coupled with large solid angles and the capacity to handle high counting rates. Our MWPC, in one of its first applications, will be backed by an array of plastic scintillators and used to study "jets" of light ions emitted in heavy-ion induced reaction.

Designed primarily to detect light ions, the MWPC contains 3 anode planes - two provide X and Y position information while the third plane is used to resolve the position ambiguity which arises when several ions traverse the chamber simultaneously. The sensitive area of the detector is 15.5 cm x 15.5 cm, the anode-cathode spacing is 6mm, and the anode wire spacing is 2.54 mm. Each anode plane consists of 64 sense wires (gold plated tungsten with a diameter of 20μ m) which are paired electrically into 32 channels. The chamber signals are handled throughout using LeCroy PCOS lll electronics. Hit-wire pulses are amplified anddiscriminated by integrated circuit cards mounted on the chamber. Logic signals from these cards are transmitted via twisted pair cable to remotely located delay and latch modules for processing.

Construction of the chamber and vacuum box has been completed and some preliminary bench tests using an electron source have been carried out.

For these tests one section of the detector was assembled, i.e. one anode plane was placed between two of the cathode planes, and a gas mixture of Argon-Ethane (50%) was flowed through the assembly. The initial test of the detector with all of the hit wires bussed together showed signals from an electron source to be well out of the noise with a gas pressure of 500 and a cathode high voltage of 3. kV. Further testing of the detector with an amplifier-discriminator card installed on the wire plane revealed the need to operate the detector in a faraday cage as the detector proved to be quite sensitive to RF noise. It is expected that the vacuum box, which will be tested in the near future, will serve as an adequate faraday cage.

High Multiplicity Array Detector Calibration

B.E. Hasselquist, G.M. Crawley, R.S. Tickle, L. Richardson, G.D. Westfall

The development of a detector array capable of detecting high multiplicity light particle events has been undertaken at NSCL. The detector consists of a triple wire plane gas counter "hit detector" backed by a phoswich ΔE-E array. Each phoswich has a thin (2mm) CaF_2 (Eu) scintillator backed by a thick (17cm) Nel02 plastic scintillator. Seven phoswich detectors comprise the full array which subtends a solid angle of 112 msr. The plastic scintillator component is a tapered hexagon in shape designed to close pack in a spherical geometry.

Six of the seven plastic scintillators were taken to IUCF to be calibrated for proton energy response from E_p=15 MeV to 120 MeV. Protons of various energies were obtained by positioning the detectors in the chamber and using a CH_2 target. A simple coincidence between a scattered proton and its recoil H target provided a clean spectrum in the detectors. Because of the large $dE/d\theta$ inherent to proton-proton scattering a Cu slit was fixed to the front of each detector. The slit was a round disk 0.350" thick with a 0.10"x0.50" slot in the center. The Cu was sufficient to stop up to 80 MeV protons, thus, the coincidence spectra consisted of a peak for protons through the slit and also in some cases a peak for protons which passed through the Cu. The beam energy of E_p=148.9 MeV was too low for scattered protons to penetrate the Cu of both detectors. The angular positions of the protons penetrating the Cu were determined by kinematics from the slit position of the coincident proton's detector.

MSUX-82-366

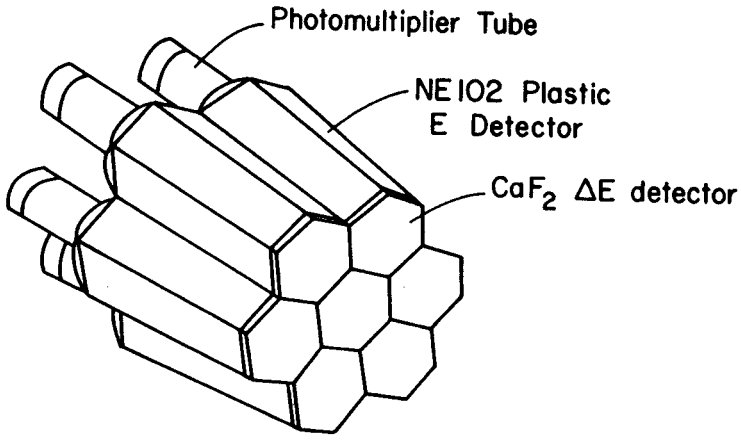

Fig. 1. Phoswich ΔE-E array.

Singles data was also taken giving peaks from ^{12}C. Peaks were found for the ^{12}C elastic and first and third excited states. The CH_2 singles also showed a peak for recoil deuterons penetrating the Cu slit. Detectors 1, 5, 6, and 7 were found to have essentially the same energy calibration, the slopes being very nearly linear and the intercepts being close to zero (see Figure 2). Detector 2 experienced a gain shift throughout the calibration, which was later found to be due to the separation of the phototube from the light guide. Detector 3 has a much different slope, but about the same intercept as the other detectors, which may indicate a different gain characteristic of the base. Overall, the energy response of the plastic scintillators was found to be quite linear.

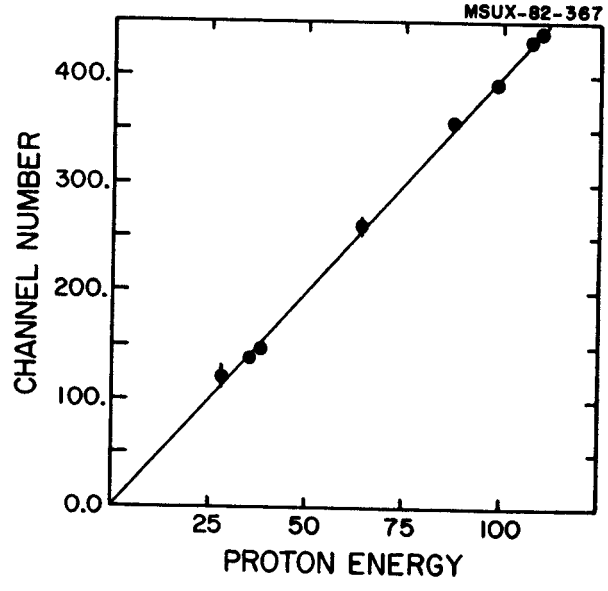

Fig. 2. Calibration curve for a representative E detector.

An experiment has been proposed and accepted by the NSCL PAC for the first scheduling period which will use the multiplicity array (Experiment #82015). At that time, normalization of the gains of the plastics with their CaF_2(Eu) ΔE components in place will be done at NSCL by recalibrating at one of the lower energies with a proton beam from the cyclotron.

Off-Line Multi-Parameter Data Analysis Program

M.B. Tsang, S. Hanchar and D. Klesch

In the past year, it has been necessary to analyze multi-parameter data off-line with VAX/750 and VAX/780 computers. In order to avoid the amount of effort associated with developing a completely new general purpose data analysis program, we have modified the multi-parameter analysis routine MUSORT[1,2] developed at the Nuclear Physics Laboratory of University of Washington, Seattle since it could be easily modified to suit our purposes.

At present, the modified version of MUSORT is a 32 parameter (it will eventually be upgraded to handle 512 parameters) general purpose sorting program. By use of a number of gating conditions either one-dimensional or two-dimensional free form gates, one is able to:

1. Presort data into disk files or on to tape.
2. Create pseudo-parameters either with functions supplied by MUSORT or by a user supplied subroutine SPCSUB.
3. Manipulate the data on an event-by-event basis using the user supplied subroutine SPCSUB.
4. Create and store on disk sorted 1-D and 2-D histograms. At present, the sorted spectra can be plotted with the TRILOG matrix printer using the plotting program HIST[3].

Further analysis with the spectra created on disk can be done with the display program MUDISP. Up to 64 MUSORT generated spectra either 1-D or 2-D can be displayed on the AED512 terminal by utilizing the general display package AED-TSK developed in NSCL. MUDISP allows one to integrate yields using free-from gates, generate gating constraints interactively for use by MUSORT and to form projections of two dimensional spectra along either X or Y axis.

One shortcoming of MUSORT is the lack of interactive display of the spectra during sorting. We are currently writing a program call MUMASTER which will allow users to interact with MUSORT and the display subroutine AED-TSK while MUSORT is sorting data and also allow communication between MUSORT and AED-TSK. The immediate goal is to allow one to utilize all the powerful features of AED-TSK to aide in the data analysis.

---

1. Nuclear Physics Laboratory Annual Report, University of Eashington, Seattle (1979), p. 164.
2. Nuclear Physics Laboratory Annual Report, University of Washington, Seattle (1980), p.212.
3. Nuclear Physics Laboratory Annual Report, University of Washington, Seattle (1980), p. 213.

Preparations for Continuation of Research Using ^{13}N as a Radioactive Tracer

P. Cornell, K. Schubert, J. Tiedje, C. Purcell, and J. Nolen

Further biological experiments are planned using ^{13}N produced with the K500 cyclotron. Initial measurements will be done to prove the feasibility of such experiments with the new cyclotron. The most productive beams for ^{13}N from the old K50 machine (25 MeV protons), will not be readily available from the new heavy ion machine. However, other reactions which may be just as productive and possibly more selective will be tried. One possibility is the fragmentation of a ^{14}N beam on a ^{9}Be target with the ^{13}N fragments being stopped in a water transfer system. Another possibility is to use a ^{13}C beam to create ^{13}N via the inverse of the (p,n) reaction, i.e., $^{1}H(^{13}C,^{13}N)n$. This could be done directly in a water target which would also stop the ^{13}N and serve as its carrier.

A new ^{13}N detector system has also been designed and a prototype has been constructed and tested. In the new system an array of proportional counters will be used to directly detect the positrons from the ^{13}N decays. These counters are relatively insensitive to the 511 keV annihilation radiation and, hence, can be used side-by-side with very little cross-talk. It is envisioned to use twelve of these detectors simultaneously in a given experiment in order to effectively process more samples during a given beam time. A schematic of a single sample in a typical experiment is indicated in Fig. 1.

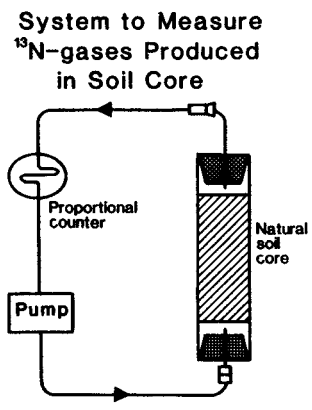

Fig. 1. Recirculating soil gas system used to detect ^{13}N gas produced by soil.

The objective of the first experiment is to measure rates of denitrification under natural soil conditions. This experiment can only be done using ^{13}N since measurement of N_2 formed from nitrate must be done in the presence of atmospheric N_2. Furthermore, the labeled nitrate added must not alter the natural nitrate concentration, and thus change the denitrification rate. In previous ^{13}N experiments we used slurries of soil, but the disruption of the natural soil structure greatly stimulated the rate of denitrification. In the planned experiments we will maintain the natural soil structure by removing natural cores of soil from the field. ^{13}N-nitrate will be added by direct injection (has been validated for ^{35}S-sulfate) or by infiltration with water simulating rainfall. The ^{13}N-N_2 and the ^{13}N-N_2O produced will be measured using the newly developed proportional counter reported above. The soil atmosphere will be continually cycled through the soil core and the detector by a membrane pump (Fig. 1). Up to 12 of these recirculating systems can be used at one time to allow additional treatments and replication.

The proportional counters are also designed to connect to the effluent stream from a gas chromatograph and a high pressure liquid chromatograph (HPLC). The former allows us to separate and quantify the ^{13}N gas species, especially N_2, NO, N_2O while the HPLC will allow us to do the same for nitrate, nitrite, and ammonium. Previously we used coincidence NaI detectors for HPLC analysis, but were limited by background and insensitivity.

The experiments on N_2 fixation are focused on determining whether the plastids are the compartments within a cell that are the site of assimilation of fixed N_2 in the soybean. Biochemical studies have suggested that ureides, which are the form in which nitrogen is transported in soybeans, are synthesized from purines in plastids. By exposing nodules to $^{13}N_2$, fractionating cell organelles, and measuring the ^{13}N in the fractions with time one can determine whether the plastids are the site of nitrogen assimilation. In later studies HPLC analysis will be used to identify the immediate products, e.g. amino acids, of nitrogen assimilation in the organelles. These experiments should also show whether purines are synthesized de novo in the plastids.

RPMS Status Report

L.H. Harwood, J.A. Nolen, S. Bricker, M.S. Curtin and E. Ormand

The past year has seen dramatic progress in the assembly of the RPMS. This progress is summarized below:

High Voltage Supplies: The PPA Cockroft-Walton and Spellman high-voltage supply are both operational and have been connected to the Wien filter.

A. PPA Supply - The PPA supply uses the Belden 8871 cable with an adapter to make the new cable fit the cable end and receptacle for the 600 kV cable. Component failure, due to their age, has been a problem. We are currently replacing many of the old components with new ones to improve the reliability of the system.

B. Spellman Supply - As was noted in last year's status report of the RPMS, a 400 kV DC supply was purchased from Spellman High-Voltage Electronics Corp. to provide voltage for one side of the electric field plates in the Wien filter. A convenient way to mount this supply was to invert it directly over one of the high-voltage inputs of the Wien filter. Unfortunately, because of space constraints, the walls of the ground cage surrounding the stack could be no farther from the toroid than 2.8". However, it was decided that filling the cage with SF_6 would allow operation at 200kV without breakdown occuring between the toroid and the cage. The final configuration of this assembly is shown in Fig. 1. Upon installation of the stack in the cage, but prior to the connection to the plates, testing was done to determine the maximum voltage attainable in air before breakdown. This was approximately 150kV, with considerable current flow via corona (on the order of 400μA). Placing 1"x13"x19" paraffin slabs between each wall of the cage and the toroid increased the breakdown voltage to 180kV and cut the current, prior to breakdown, in half. The best results were gained when the wax blocks were touching each other, leaving no gaps between the toroid and the walls. The results of these tests are summarized in Fig. 2. Thin walls of some other dielectric materials (glass, FEP, Mylar) were tested; while these also significantly lowered the current flow via corona, breakdown occured at voltages equal to or below that of air alone. Consequently, the toroid was coated with wax (to a maximum thickness of 3/4") and 1 1/4" thick blocks were cast to surround it. With this configuration, breakdown occured at 240 kV, allowing us a reasonable safety margin for running at the anticipated maximum voltage of 200 kV on the each plate and also eliminating the need to fill the cage with SF_6.

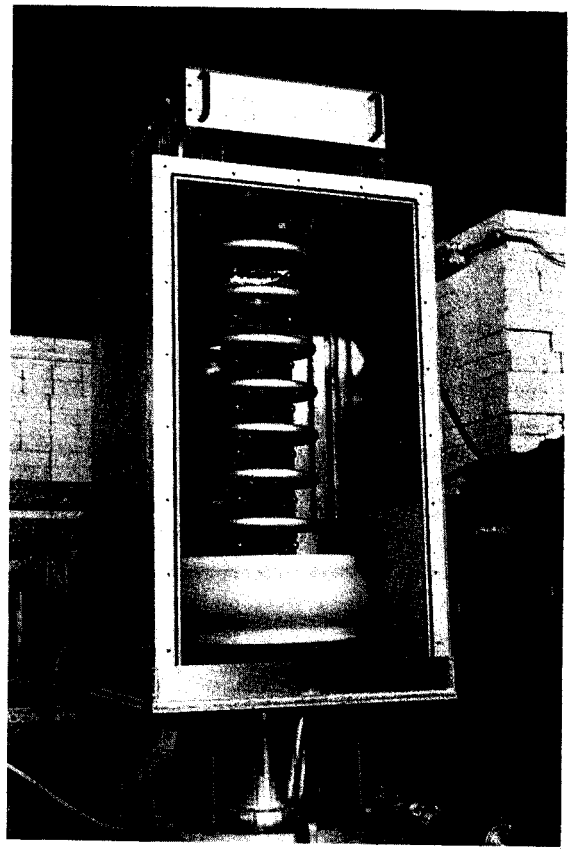

Fig. 1. Photograph of Spellman H.V. supply surrounded by wax in its shielding cage.

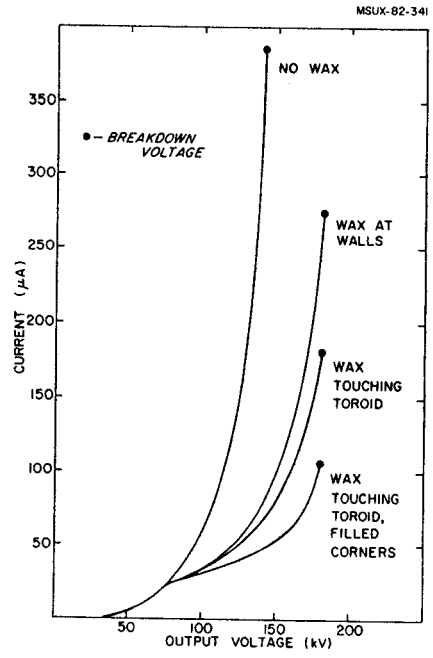

Fig. 2. Graphs of leakage currents vs. voltage for the Spellman supply under different conditions. Each curve terminates at the breakdown voltage for that configuration. See text for further explanation.

Since connecting the Spellman to the plates, the supply has only been operated up to 160 kV. However, no difficulty is foreseen in bringing the Spellman up to 200 kV when the other components of the RPMS are ready.

High Voltage Tests: We are glad to report that the voltage tests on the Wien filter have gone as high as 300 kV, limited only by a component failure (attributed to age) within the PPA supply. The voltage supplies were operated at equal voltages, i.e. 150 kV at the time of the failure. The Spellman showed no signs of problems. The Wien filter showed no unexpected conditioning phenomena; we anticipate that we will have little trouble surpassing the 300 KV (30 kv/cm) point at the next test.

Magnetic Tests: The University of Maryland magnet supply has been installed and has successfully run the Wien filter magnet at 600 A.

Mechanical Construction and Assembly: All major structural components for the system are in place. The carriage was installed, and the quadrupole doublet and Wien filter mounted on it; the Cornell magnet was mounted on its pivot bearings and connected to the carriage. One can easily rotate the system with hand-pressure on the carriage at the Wien filter entrance. The screw-drive hoist mechanism for raising and lowering the "tail" of the RPMS has also been installed.

Presently under construction are the target chamber, the two moveable vacuum chambers, and the solid angle aperture mechanism. The target chamber is essentially finished, and all the parts are in-house for the vacuum box for the inflector magnet. With the installation of these parts and the aperture box at the exit of the Wien filter, the RPMS will be complete.

Detectors: A small 2-dimensional wire counter has been designed and constructed for initial measurements at the RPMS focal plane. It is described in the detector lab section of this annual report. In addition to this detector, a solid state detector telescope has been acquired for use in early experiments. The telescope will be used to stop and identify heavy ion reaction products. The telescope will be mounted inside a NaI annulus which will detect gammas from the decay of the stopped isotopes.

Progress in Construction of the k=320 Spectrograph

S. Bricker, R. Blue, and J. Nolen, Jr.

The construction of the k=320 spectrograph (S320) is nearly complete. The floor plan of this spectrograph is shown in the figure. The pivot bearing, carriage, rail, and drive system are all complete. All major components, scattering chamber, quadrupole doublet, dipole, multipole and sextupole, exist and are in position on the carriage. Modifications to the dipole vacuum box are complete and it is currently under vacuum with a Varian 8" cryopump. A new target ladder and target motion system, including a vacuum lock, have been designed for the Minnesota chamber, and shop work is nearing completion. This system is compatible with our standard frames (2" wide x 1-1/8" tall x 1/16" thick), vacuum lock transfer system, and spectrograph remote control and readout system. A general purpose focal plane detector case has been constructed and a focal plane detector is currently being tested (see separate report by Lynch and Yurkon in detector lab section). The iron pieces to change the entrance curvature of the dipole from concave to convex have been machined and are glued in place. An octupole magnet to be positioned between the dipole and sextupole has been constructed and is currently being tested (see separate report). The solid angle defining apertures for this spectrograph will be located approximately 2m from the target at the entrance of the first quadrupole. For a solid angle of 0.5 msr the aperture is approximately 2 inches square. The aperture holder and remote positioning system for four different machined apertures has been designed and is currently under construction. The four apertures can be removed and replaced by different ones via a port in the side of the aperture holder mechansim. Miscellaneous items such as an active collimator, Faraday cups, and beam monitors are being designed by several users. Preliminary testing of the S320 should take place in early 1983.

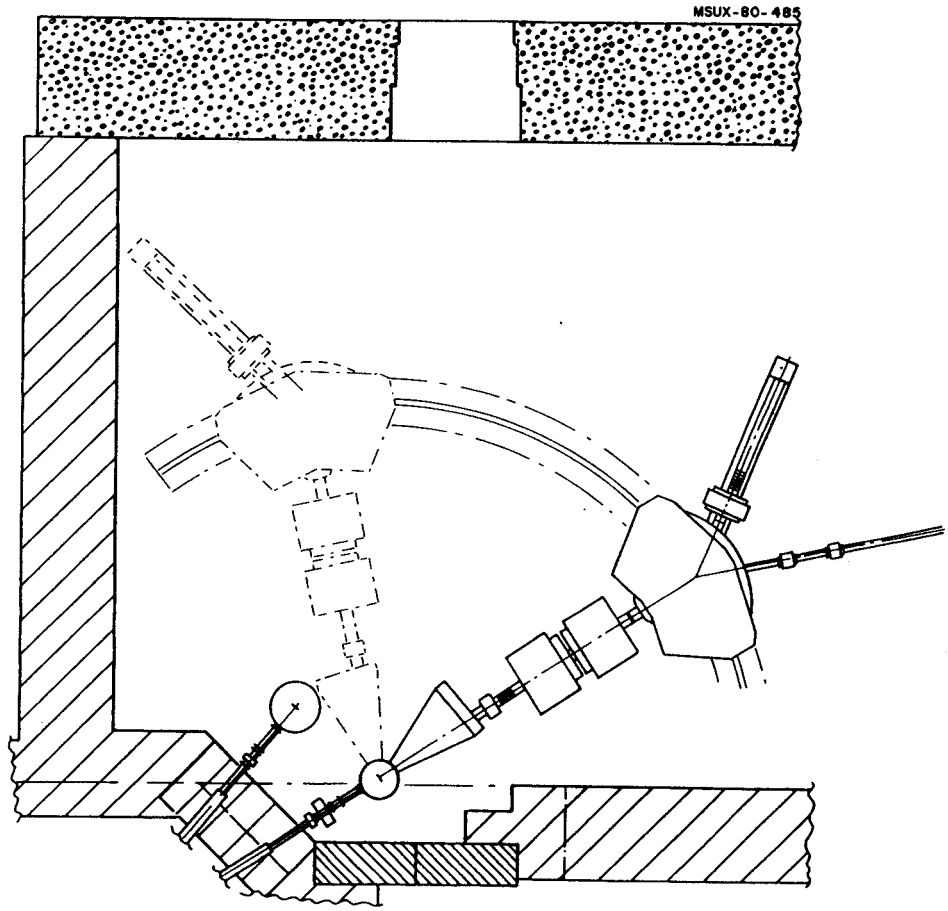

Fig. 1. Plan view of the S320 spectrograph.

Raytracing Calculations of the S320 with the program MOTOR

B. Sherrill, T. Coffman and J. Nolen, Jr.

Detailed raytracing calculations of the S320 spectrograph have been performed using the computer code MOTER.[1] These calculations were done to optimize the dipole entrance curvature and sextupole field strength to obtain maximum p/Δp. The effects of beam momentum dispersion on target for the purposes of running the spectrograph in the energy-loss mode and quadrupole tuning to correct for reaction kinematics were included in the calculations. Incoherent beam spot size was not included in the calculations. However, we expect the spectrograph linewidth will be no better than the incoherent spot size times the spectrograph magnification (M_x=.67), but this effect will have to be checked by measurements with the Phase I cyclotron beam. The incoherent spot size from the old K-50 cyclotron was less than 0.1 mm.

The S320 spectrograph component layout and beam envelopes are shown in Fig. 1 for reference. Two sets of calculations were performed. One with the originally proposed QQDS configuration with 0.3 msr solid angle, and one with a multipole added to give a QQDMS configuration with 0.5 msr solid angle. All calculations assumed an energy acceptance range of 20% for 320 MeV ^{4}He particles, an energy-dispersed horizontal spot size on target of 2 mm, and a vertical spot size of 3 mm.

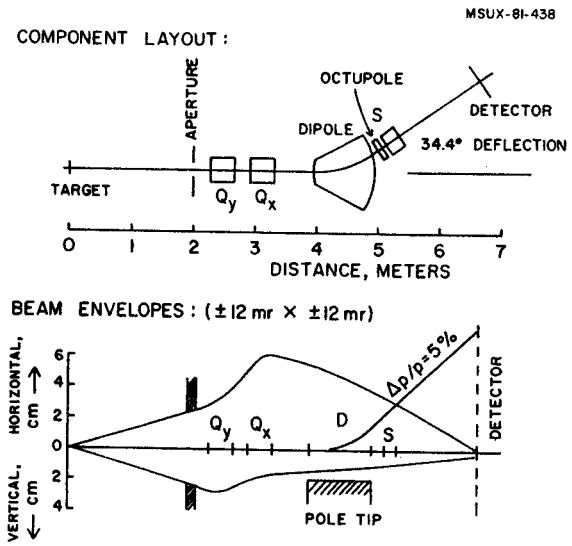

Fig. 1. Schematic diagram of the S320 spectrograph. Shown is the component layout, and beam envelopes.

MOTER evaluates the aberration limited momentum resolution by calculating the focal-plane position/momentum dependence of the beam phase space. This is done by fitting the focal-plane position with a polynomial in powers of momentum (or vise-versa). The residual error, i.e. the difference in a ray's actual raytraced position and the polynomial-fitted position represents the spectrograph aberration since the position/momentum dependence of the focal plane will be known. Thus, the entire spectrograph energy range can be sampled simultaneously and the intrinsic spectrograph resolution evaluated by the width of the resulting error-function. Fig. 2 is a sample calculation using the QQDMS configuration showing a histogram of ray number, for 200 randomly generated rays, versus momentum error function. The distribution is fitted with a gaussian and the resulting FWHM yields p/Δp=3500 for the spectrograph running in the energy loss mode with a beam energy spread of 0.10%.

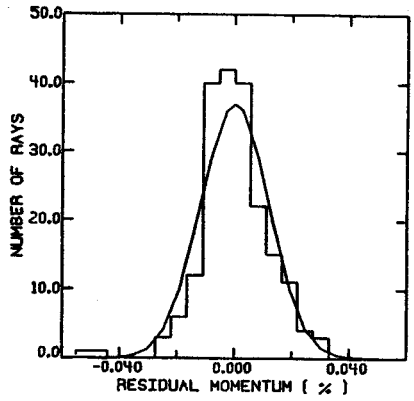

Fig. 2. Results of a sample MOTER calculation.

MOTER optimizes the specified parameters to minimize the error function line width. A comparison of the optimized parameters with and without the multipole are shown in Table I.

Table I.

PARAMETER	OPTIMIZED VALUE	
	QQDS	QQMDS
Y-QUAD (kG)	-8.55	-8.55
X-QUAD (kG)	7.14	7.17
SEXTUPOLE (kG)	1.99	2.07
DIPOLE ENTRANCE CURVATURE (cm)	69.0	68.5

The momentum resolution was also calculated as a function of the beam momentum dispersion on target. The results are shown in Fig. 3 for the two cases. In the .3 msr and the .5 msr cases the optimum dispersion on target, δ_{target} was almost exactly the predicted theoretical value obtained from requiring

$$x_{targ} = \frac{D_s}{M_x} \delta_{targ}$$

where x_{targ} is the horizontal position on target, D_s is the spectrograph dispersion, M_x the spectrograph magnification, and δ_{targ} is the momentum deviation (in %) of the beam from the central momentum. The addition of the multipole field was seen to increase the required dispersion by approximately 2%.

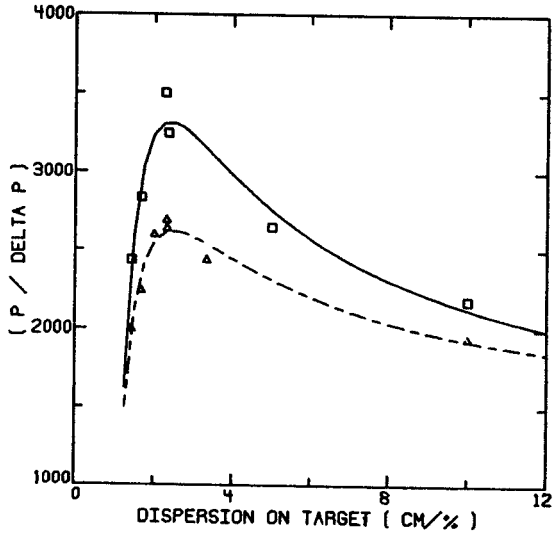

Fig. 3. Plots of the optimum dispersion-on-target search with and without the multipole. The solid line is the .5 msr case, the dashed line is the .3 msr case.

Finally, kinematic effects were taken into account and corrected using the optimizing features of MOTER. To correct for a given $k = -(1/p)\frac{dp}{d\theta}$ the focal plane had to be moved, or the quadrupole fields varied. In our case MOTER was allowed to retune the x-quadrupole. It was found unnecessary to retune the y-quad. The results for the two cases are shown in Fig. 4. We found a linear relationship between the k parameter and the required percentage change in the x-quadrupole strength (See Fig. 5).

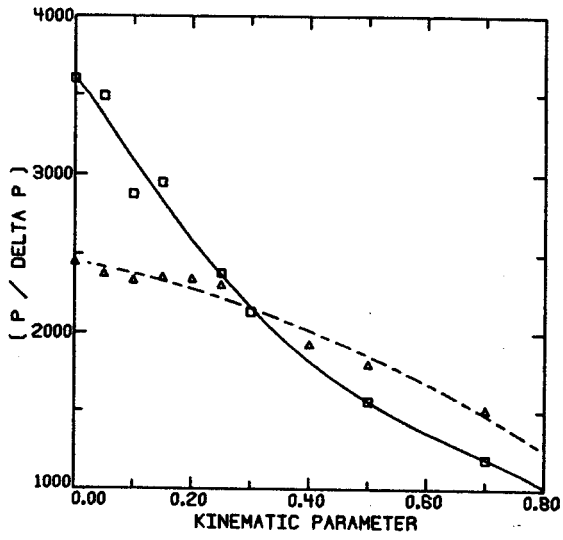

Fig. 4. Calculated effects of reaction kinematics. The dashed line is the .3 msr case. The poorer resolution of the QQDMS configuration at large k is due to the larger solid angle.

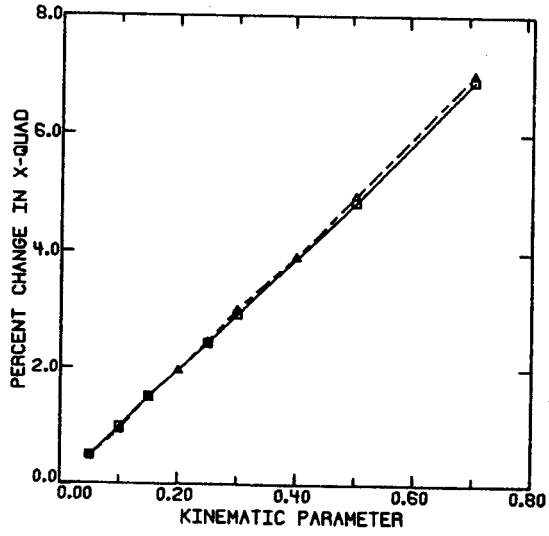

Fig. 5. Plotted is the percent change in the x-quad needed to reoptimize the spectrograph. The dashed line is the .3 msr case and the solid line is the .5 msr case.

Eventually, the above calculations will be checked with cyclotron beams to determine the agreement with actual experimental conditions.

1. H.A. Thiessen, M.M. Klein, and K.G. Boyer, LASL Report, April 1979 (unpublished).

Construction of a Non-Circular Current-Sheet Octupole Magnet

B. Sherrill, N. Kedarnath and J. Nolen, Jr.

The design of a non-circular octupole magnet for use in the S320 spectrograph was presented in last year's annual report. The construction of that magnet is now complete and it is shown in the photograph below (Fig. 1) The measured parameters of this magnet are given in the table, while the calculated vs. measured field is plotted in Fig. 2. The geometrical constraint of fitting between the coil of the dipole magnet dictated the unusual geometry of this magnet. As a result the magnet was wound in 4 identical sections using 1/8" square hollow copper conductor. Due to the complicated nature of the coil the conductor was wound directly on the magnet iron.

The calculated resolution and solid angle of the S320 spectrograph are both improved through the addition of this octupole to the system. This magnet is actually a multipole as indicated in Table I. It is dominantly octupole combined with about 30% dodecapole. This combination improves the calculated resolution of the spectrograph more than a pure octupole. These improvements are given in a separate section of the annual report.

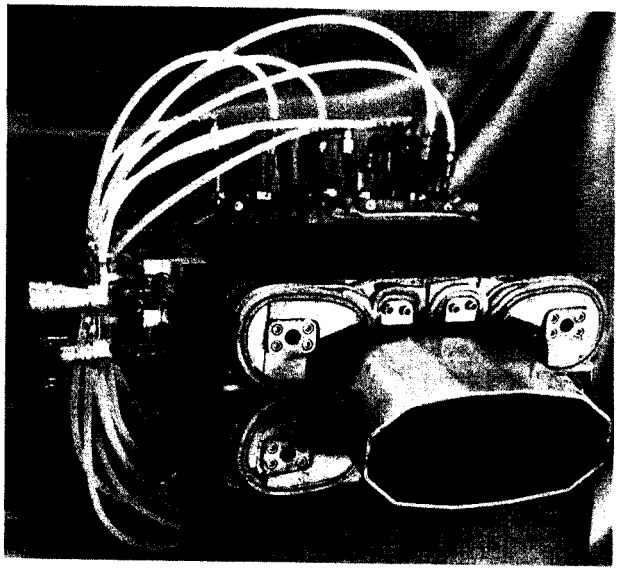

Fig. 1. Photograph showing the completed magnet and water cooling lines.

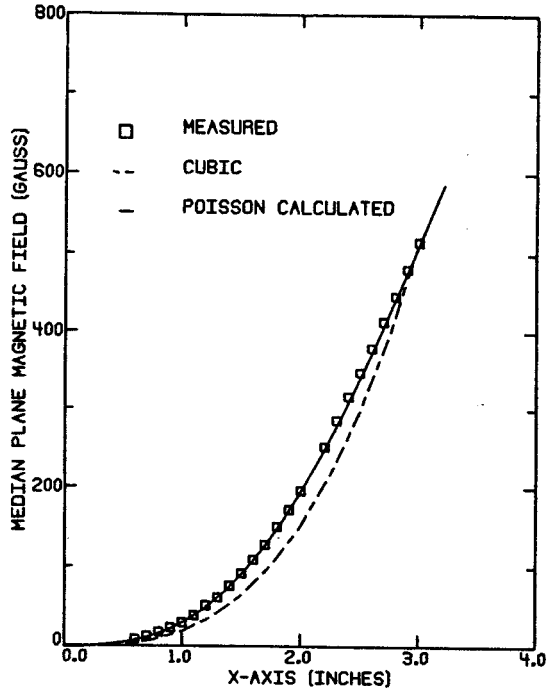

Fig. 2. Plot of the POISSON calculated vs. measured median plane magnetic field. For reference, a true octupole field is also plotted.

Table 1: Parameters measured while running the magnet at a field of 514G at r=3.0".

MAGNET PARAMETER	VALUE	
Multipole Composition		
QUAD	-8.3	G
OCTA	-736.3	G
DODEC	266.7	G
16 POLE	33.4	G
20 POLE	-31.5	G
CURRENT	102.0	A
VOLTAGE	16.6	Volts
COOLING WATER FLOW RATE (for 8 sections of 30.0' long 1/8" square copper conductor through a 1/16" square hole)	.75	gal/min.

Final Optical Design for the S800

A.F. Zeller, L.H. Harwood and J.A. Nolen

The design philosophy for the S800 large-acceptance-high resolution spectrograph has evolved from correction of aberrations by second and higher order dipole edge curvatures and multipole winding in quadrupoles to one of simple optical design, with the need for trajectory reconstruction based on focal plane detector measurements. The advantage of a single focal plane detector, requiring fewer computer operations, is overcome by the necessarily complex curvatures and multipoles needed to correct the aberrations. Although a perfect second order solution can be found, the induced higher-order aberrations[1] require corrections through fifth order. It was not possible to meet the resolution requirements[2,3] of $E/\Delta E=10^4$ and $\Delta\phi$=1 mr over the full solid angle and energy band pass ($\pm$5%) while at the same time compensating for beam energy spread by keeping the system in a dispersion matched mode. Thus the philosophy of correction for aberrations at the focal plane by using two x-y position sensitive detectors with active ray tracing was adopted. A brief summary of design parameters is listed in Table I.

Table I

Element	Parameters (Bρ = 1.2 GeV/C)
Q1	40 cm long, 10 cm radius, 21 kG pole tip field
Q2	40 cm long, 17 x 35 cm^2, 10 kg pole tip field
D1	3.5 m long, 15 cm gap, ρ = 2.67 m, 15 kg field, 75° bend angle, normal entrance edge angle, 30° exit edge, mass ≈70 tons
D2	identical to D1 except entrance is 30°, exit is normal
Focal plane	52 x 15 cm^2

In order to determine whether the system could meet the design goals, the optimizing ray trace program MOTER[4] was used. Approximately 25 aberration coefficients, ranging from simple second order terms such as x/θ^2 and $x/\theta\delta$ up to complicated fifth order ones, were corrected for in both momentum and scattering angle "measurements". Realistic measurement errors on x, y, θ and φ at the focal plane were used to calculate the residual error in the "measured" momentum and scattering angle. The error histograms for the resulting momentum and angle "measurements" at a solid angle of 10 msr, ±2.5% momentum bandpass are shown in Figs. 1 and 2, respectively. The corresponding FWHM energy resolution is 1 part in 10^4 and the angular resolution is 0.7 mr. Listed in Table II are typical resolutions for some solid-angle/momentum range combinations. These may vary by 10-20% depending on the random rays chosen by the program and by whether momentum or scattering angle is better optimized.

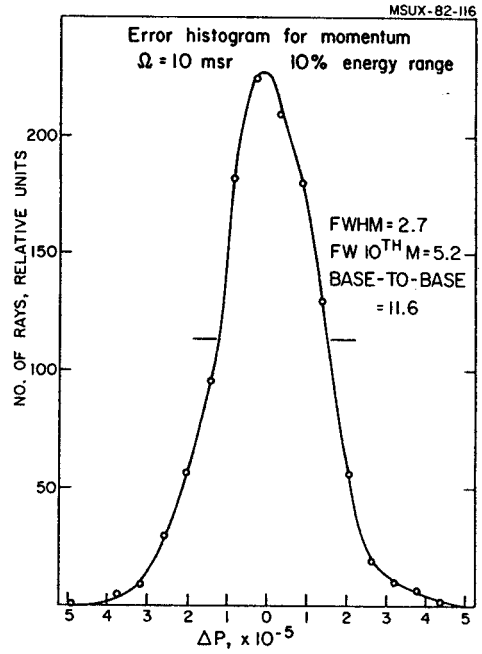

Fig. 1. Error histogram for momentum.

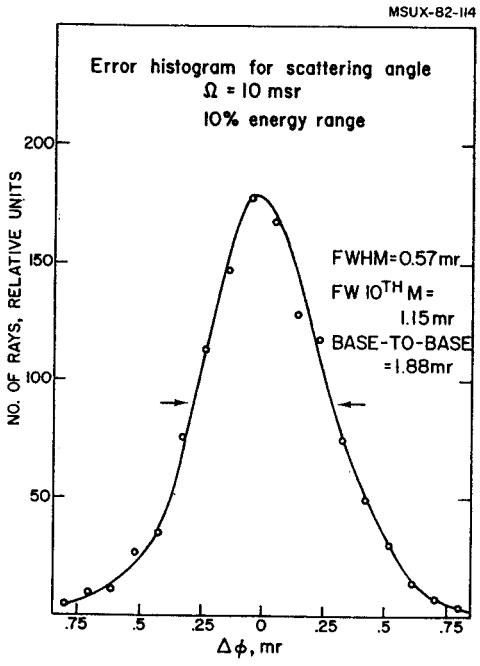

Fig. 2. Error histogram for scattering angles.

Table II

Nominal Solid angle (msr)	θxφ (mr^2)	band pass Δp/p (%)	ΔE/E FWHM ($x10^{-4}$)	ΔE/E Base-to-Base ($x10^{-4}$)	Δφ FWHM (mr)	Δφ Base-to-Base (mr)
3	15x180	±2.5	0.5	1.5	0.7	2.3
10	60x180	±2.5	1.0	2.3	0.7	2.3
20	120x180	±0.25	1.0	1.8	0.8	4.4
20*	120x180	±2.5	1.0	4.0	0.8	4.4

*Slits limit the rays thru the dipoles to a width which corresponds to the maximum radius for the 10 msr, ±2.5% solution, resulting in a band pass which drops to 15 msr at the extreme of the momentum range.

Thus the design goals of $\Delta E/E = 1 \times 10^{-4}$ at 10 msr and full 10% energy range and an angular resolution of 1 mr is achieved for a device with no multipole elements but with active ray tracing at the focal plane.

1. L. Harwood and J. Nolen, MSU Annual Report 1980-81, p. 100.
2. MSU Annual Report 1979-80, p. 78.
3. ibid, 1978-79, p. 102.
4. H.A. Thiessen, M.K. Klein and K.G. Boyer, LASL Report, 1979 (unpublished).

H-Magnet Design Studies for the S800

A.F. Zeller and J.A. Nolen

Dipole design studies for the S800 spectrograph in previous reports[1,2] have concentrated on a window-frame dipole design, which, although the most compact design for a given volume of good field (a gradient of $\pm$ 1G/cm), requires a complex superconducting saddle coil. The important comparison, then, between the window-frame geometry and the H-frame is the trade-off between a smaller magnet and complexity of coil structure.

A study analagous to that done for the window-frame geometry[2] was made on an H-frame magnet for the S800 spectrograph using the code POISSON.[3] Two strategies were used to maximize the region of good field: 1) improving the infinite permeability solution, and 2) improving the finite permeability solution. The infinite permeability solution is improved by the addition of a trim coil on the median plane with current in the same direction as the main coil. Because the field in an H-frame magnet decreases as the edge of pole tip is approached, a coil on the median plane has the effect of keeping the field from decreasing as rapidly. The addition of the return coil directly above, on the pole tip, also improves the field profile and makes assembly easier. The trim coils are normal conductors, carrying approximately 0.7% of the main coil ampere-turns. The effects of the trim coils on the infinite permeability solution are shown in Fig. 1 and 2, along with a profile for the gap region showing the position of the trim coils. Fig. 1 shows the ratio of the field to the central field, in parts per 10^5. Fig. 2 shows the gradients. The trim coils add an additional 5 cm of good field.

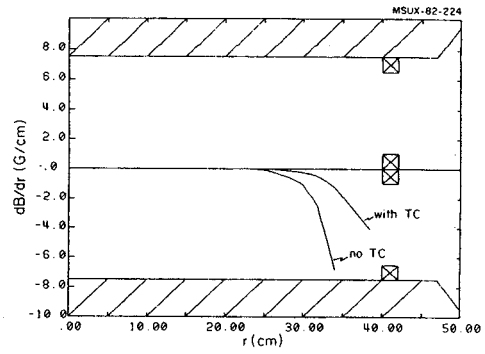

Fig. 2. Calculated field gradients for infinite permeability solutions with and without trim coil

The field profile is kept reasonable over a wide dynamic range (with finite permeability) by using a tapered gap behind the pole tip which is 1 cm high at the midline and 1/2 cm at a distance of 40 cm. It does not extend all the way across the pole. The gradients for the 15 kG solution, with and without the filter are shown in Fig. 3. The field profile, shown in Fig. 4, demonstrates the effects more dramatically than the gradients. The gradients, normalized to 15 kG, for excitations from 7 to 16 kG are shown in Fig. 5. Corresponding field profiles are shown in Fig. 6.

Changing the design to an H-frame has the advantage of reducing the forces on the coil, since the coil is in a region of lower magnetic field. This reduces the radial forces on the coil by a factor of almost five, considerably reducing the required thickness of the support structure and the related conduction heat load.

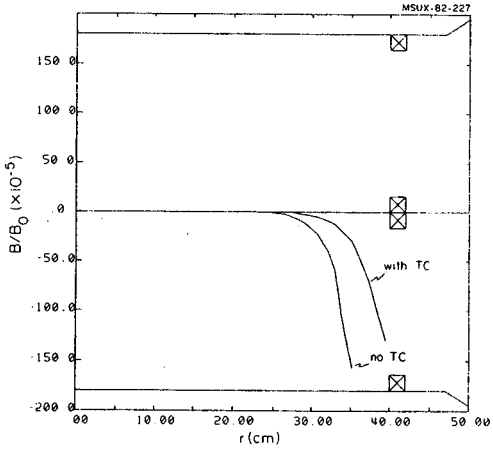

Fig. 1. Calculated field profiles for infinite permeability with and without trim coil.

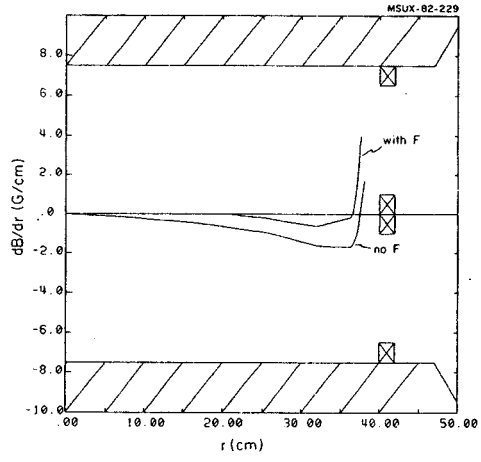

Fig. 3. Calculated field gradients for the 15 kG finite permeability solution with and without the filter.

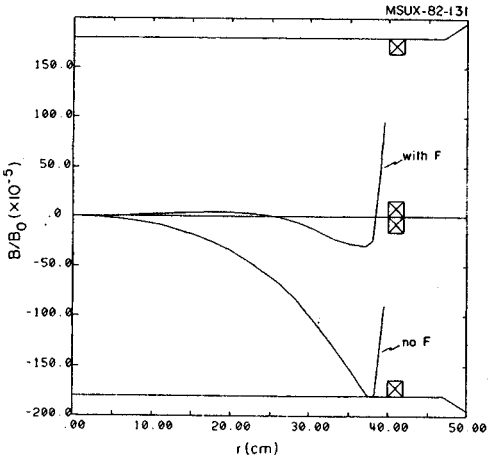

Fig. 4. Calculated field profiles at 15 kG with and without the filter.

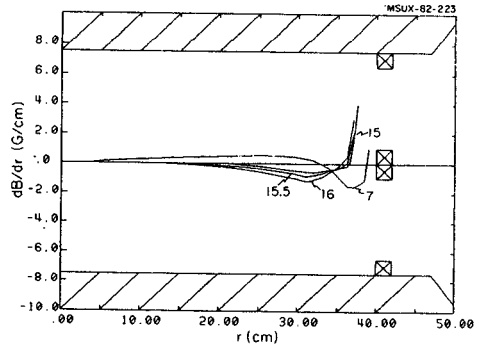

Fig. 5. Field gradients for 7 to 16 kG.

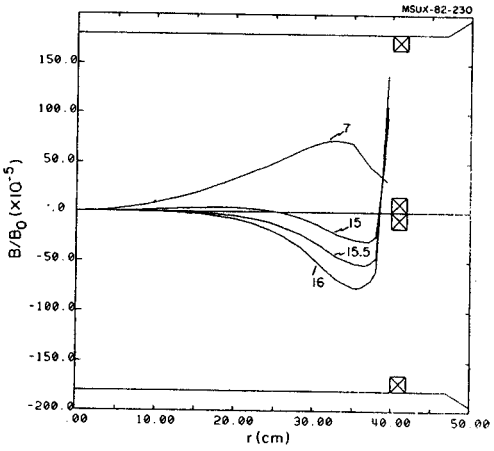

Fig. 6. Field profiles for 7 to 16 kG.

Additionally, the lowered force reduces the tendency for conductor motion. It turns out that the calculated radial forces peak for an excitation of 15 kG, as shown in Fig. 7. This allows the possible operation at higher fields without worrying about the failure of the radial support structure. The axial (y) forces are balanced internally within the bobbin which contains both the upper and lower coils.

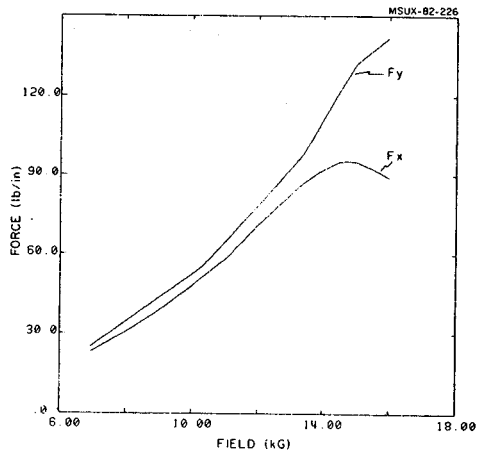

Fig. 7. Radial (F_x) and axial (F_y) forces on the S800 coil, per inch of coil length.

The biggest advantage of the H-frame is not having to produce a very complicated saddle coil, especially since the preliminary design for the H-frame coil is still complex. The cost of the H-frame design vis-a vis the window-frame is the mass increase from 50 tons to 70 tons. This represents an approximate increase in steel costs of $60,000 per dipole. We feel, however, that the simplified coil and bobbin design more than offset this cost.

1. MSU Annual Report 1979-80, p. 78 (unpublished).
2. ibid, 1980-81, p. 105.
3. R.F. Holsinger, program POISSON (unpublished).